The mating-type and pathogenicity locus of the fungus *Ustilago hordei* spans a 500-kb region

Nancy Lee*, Guus Bakkeren*†, Katherine Wong*, John E. Sherwood‡, and James W. Kronstad*§

*Biotechnology Laboratory, Departments of Microbiology and Immunology, and Faculty of Agricultural Sciences, University of British Columbia, Vancouver, BC, Canada V6T 1Z3; and ‡Department of Plant Sciences, Montana State University, Bozeman, MT 59717-3150

Communicated by R. James Cook, Washington State University, Pullman, WA, November 3, 1999 (received for review July 16, 1999)

The fungal pathogen *Ustilago hordei* causes the covered smut disease of barley and oats. Mating and pathogenicity in this fungus are controlled by the *MAT* locus, which contains two distinct gene complexes, *a* and *b*. In this study, we tagged the *a* and *b* regions with the recognition sequence for the restriction enzyme I-*Sce*I and determined that the distance between the complexes is 500 kb in a *MAT-1* strain and 430 kb in a *MAT-2* strain. Characterization of the organization of the known genes within the *a* and *b* gene complexes provided evidence for nonhomology and sequence inversion between *MAT-1* and *MAT-2*. Antibiotic-resistance markers also were used to tag the *a* gene complex in *MAT-1* strains (phleomycin) and the *b* gene complex in *MAT-2* strains (hygromycin). Crosses were performed with these strains and progeny resistant to both antibiotics were recovered at a very low frequency, suggesting that recombination is suppressed within the *MAT* region. Overall, the chromosome homologues carrying the *MAT* locus of *U. hordei* share features with primitive sex chromosomes, with the added twist that the *MAT* locus also controls pathogenicity.

MAT locus | sex chromosome | smut disease | phytopathogen | basidiomycete

Ustilago hordei represents a group of fungal pathogens that cause economically important smut diseases on small-grain cereals (1). These fungi grow as hyphae within developing seedlings without causing symptoms; upon flowering of the host plant, the fungal cells proliferate and form masses of dark teliospores that replace the seeds. The diploid teliospores germinate and undergo meiosis to yield haploid cells. These meiotic progeny must mate to infect the host, and infection is a prerequisite for completion of the sexual phase of the life cycle, i.e., the formation of teliospores. Sex and pathogenicity therefore are interconnected in *U. hordei* and related smut fungi, and the mating-type genes are considered pathogenicity factors.

U. hordei has a bipolar mating system controlled by one mating-type locus (*MAT*) with two alleles or alternative specificities, *MAT-1* and *MAT-2.* DNA hybridization experiments with the well-characterized *a* and *b* mating-type genes from the related species, *Ustilago maydis,* revealed that *U. hordei* possesses similar mating-type functions located at so-called *a* and *b* gene complexes within the *MAT* locus (2, 3). In contrast to *U. hordei*, *U. maydis* has a tetrapolar mating system because the *a* and *b* loci are on separate chromosomes and therefore segregate independently during meiosis (3, 4). Thus, the tetrapolar and bipolar mating systems are distinguished by differences in the genomic organizations of the *a* and *b* genes (3). In *U. maydis*, two specificities exist for the *a* locus: *a1* and *a2* (5, 6). The *a* locus encodes cell-type specific pheromones (*mfa*) as well as the pheromone receptors (*pra*) that recognize pheromones from compatible mating partners. The *b* locus of *U. maydis* is multiallelic and contains two divergently transcribed genes, *bE* (*b*East) and *bW* (*b*West) (4, 7–9). The *b* locus controls pathogenicity and completion of the life cycle through self vs. nonself recognition between bE and bW polypeptides to establish a regulatory factor (8, 9). The homologues of the *a* and *b* genes from *U. maydis* and *U. hordei* are conserved in structure and function (2, 3, 10–12). In both species, only cells of opposite mating type, that is, having different specificities at both *a* and *b*, successfully mate and form colonies with aerial hyphae (fuz^+ reaction); these combinations are infectious when inoculated into host plants. Conversely, haploid strains or incompatible partners of the same mating type form yeast-like colonies and are noninfectious.

Previous studies have shown that *a* and *b* are physically linked on the largest chromosome of *U. hordei* and, together, they encode key functions within the *MAT* locus (3). In this report, we describe the construction and analysis of strains tagged at the *a* and *b* gene complexes to determine the size of the *MAT* locus. Specifically, we show that the *MAT* locus extends over a large region and that the size and organization of the locus differs between *MAT-1* and *MAT-2* strains. In addition, we use the tagged strains to further demonstrate that the region between the *a* and *b* gene complexes is suppressed for recombination.

Materials and Methods

Strains and Media. Strains used in this study are listed in Table 1. Fungal strains were grown and mating tests were performed as described (12, 13).

Plasmid Constructions and Gene Complex Tagging. The four constructs used to tag the *a* and *b* gene complexes in *U. hordei* were based on the two plasmids, pSceI-Hyg#1 and pSce-phleo#4. The hygromycin B resistance cassette (14) and two annealed oligonucleotides containing the I-*Sce*I recognition sequence (5′-TAGGGATAACAGGGTAAT-3′) were cloned into plasmid pGEM3+ (Promega) to construct pSceI-Hyg#1. Plasmid pSce-phleo#4 was constructed by substituting the hygromycin B resistance cassette of pSceI-Hyg#1 with the phleomycin resistance cassette from pUble10 (15). I-*Sce*I is an intron-homing enzyme from *Saccharomyces cerevisiae* (Boehringer Mannheim; ref. 16).

The *a1* gene complex of *U. hordei* strain 4857–4 and the *a2* gene complex of *U. hordei* strain 365–57 were tagged with the phleomycin-I-*Sce*I cassette from pSce-phleo#4, creating strains 364–62/364–86 and 365–57dt51, respectively (Table 1; Fig. 1). The *b1* gene complex of *U. hordei* strain 364–86 and the *b2* gene complex of *U. hordei* strain 4857–5 were tagged with the hygromycin B-I-*Sce*I cassette of pSceI-Hyg#1, creating strains 364–86dt21 and 365–57/365–71, respectively (Table 1; Fig. 1). Details about DNA constructs can be obtained from the authors. *U. hordei* electrotransformation and genomic DNA isolation were

Abbreviations: *MAT*, mating-type locus; CHEF, clamped homogenous electric field; drp, double-resistant progeny.

†Present address: Agriculture and Agri-Food Canada, Pacific Agri-Food Research Centre, Summerland, BC, Canada, V0H 1Z0.

§To whom reprint requests should be addressed at: Biotechnology Laboratory, 237-6174 University Boulevard, Vancouver, BC, Canada V6T 1Z3. E-mail: kronstad@interchange.ubc.ca.

The publication costs of this article were defrayed in part by page charge payment. This article must therefore be hereby marked "*advertisement*" in accordance with 18 U.S.C. §1734 solely to indicate this fact.

Table 1. *U. hordei* strains

Strain	Genotype*	Source
U. hordei 549	*a2b1* (Δ*b2*, *UhbWE1*, *hyg*^{r}, *phleo*^{r})†	(11)
U. hordei 550	*a2b1* (Δ*b2*, *UhbWE1*, *hyg*^{r}, *phleo*^{r})†	(11)
U. hordei 551	*a1b2* (Δ*b1*, *UhbW2*, *hyg*^{r}, *phleo*^{r})†	(11)
U. hordei 552	*a1b2* (Δ*b1*, *UhbW2*, *hyg*^{r}, *phleo*^{r})†	(11)
U. hordei 4857-4	*a1b1* (wild-type strain)	P. Thomas (11)
U. hordei 4857-5	*a2b2* (wild-type strain)	P. Thomas (11)
U. hordei 364-62/364-86	*a1b1* (Δ*pan1*::*phleo*^{r}/*Sce*I)‡	This work
U. hordei 364-86dt21	*a1b1* (Δ*pan1*::*phleo*^{r}/*Sce*I, Δ*bWE1*:*hyg*^{r}/*Sce*I)§	This work
U. hordei 365-57/365-71	*a2b2* (Δ*bW2*::*hyg*^{r}/*Sce*I)¶	This work
U. hordei 365-57dt51	*a2b2* (Δ*bW2*::*hyg*^{r}/*Sce*I, Δ*pan1*::*phleo*^{r}/*Sce*I)‖	This work

*phleo^r, phleomycin resistance; hyg^r, hygromycin B resistance; *Sce*I, I-*Sce*I recognition sequence.
†In these strains, the resident *b* genes were inactivated by insertion of a hygromycin B resistance marker; subsequently, functional *b* gene complexes (pUhbWE1 or pUhbW2) were integrated at ectopic sites (11).
‡These strains were constructed by transformation of strain 4857-4 with pSce-phleo#4 at *a1*.
§This strain was constructed by transformation of strain 364-86 with pSceI-Hyg#1 at *b1*.
¶These strains were constructed by transformation of strain 4857-5 with pSceI-Hyg#1 at *b2*.
‖This strain was constructed by transformation of strain 365-57 with pSce-phleo#4 at *a2*.

performed as described (2, 10). Homologous integration of transforming DNA was confirmed by DNA hybridization (data not shown).

Pulse-Field Gel Electrophoresis and Hybridization Analysis. Chromosome-sized DNA from *U. hordei* was prepared and digested with I-*Sce*I essentially as described (16). Agarose plugs were loaded into 1.2% (wt/vol) agarose gels in 0.5× TBE buffer (45 mM Tris-Borate/1 mM EDTA). Gel electrophoresis was performed at 16°C by using a contour clamped homogenous electric field (CHEF) electrophoresis apparatus (CHEF-DR II, Bio-Rad) under the following conditions: 45-sec pulse at 150 V for 48 hr (Figs. 2 and 3*D*), 45-sec pulse at 200 V for 48 hr (Fig. 3*A*), or 3,600-sec pulse ramped to 600-sec pulse at 60 V for 120 hr and 600-sec pulse ramped to 96-sec pulse at 60 V for 50 hr (Fig. 4). The gels were stained with ethidium bromide and treated with 0.25 M HCl, and the DNA was transferred to nylon membranes (Hybond-N+, Amersham Pharmacia). DNA fragments for hybridization probes were selected based on their proximity to the engineered I-*Sce*I sites. For all hybridizations, the probes were labeled with [α-^{32}P]dCTP by random-priming (Amersham Pharmacia). Prehybridizations and hybridizations were in 7% SDS, 0.5 M Na_2HPO_4 at 65°C, and membranes were washed as described (3).

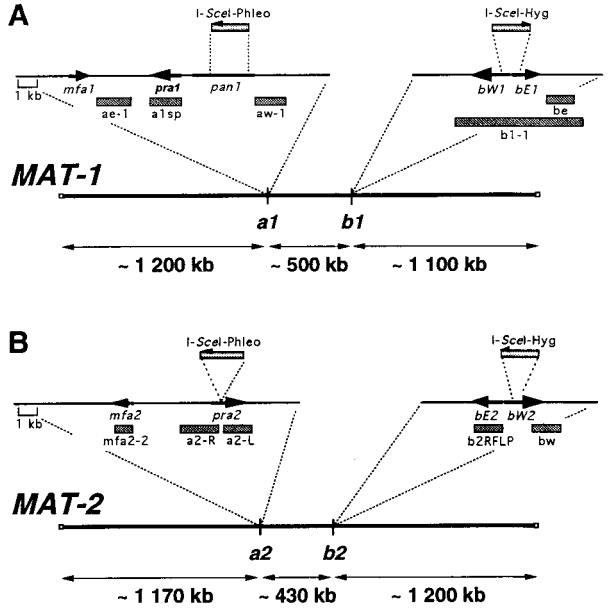

Fig. 1. Chromosomal organization of the *MAT-1* (*A*) and *MAT-2* (*B*) loci. The two thick lines represent the *MAT* chromosomes. The thin lines represent inserts of plasmid constructs used to tag the respective mating-type loci. The *mfa, pra, bE*, and *bW* ORFs are shown as black boxed arrows denoting the direction of transcription. The direction of transcription of *pan1* and its location in *MAT-2* are not known. The locations of probes used for the hybridizations are shown as gray bars. For details on the organization of the gene complexes, see ref. 17.

Plant Inoculation and Teliospore Isolation. Barley seedlings (*Hordeum vulgare* L.) of cultivars Odessa and 66–2 (gift from P. Thomas, Argiculture and Agri-Food Canada, Winnipeg, MB, Canada) were inoculated with compatible haploid strains of *U. hordei* as described (11). Teliospores were sterilized with 0.06% sodium hyperchlorite, washed in sterile water, and germinated on Difco potato dextrose agar (PDA). Diploid teliospores were spread on 20 Petri plates to a density of approximately 5,000 teliospores/plate. Metabasidia possessing an average of 12 haploid sporidia were collected from the PDA plates and resuspended in potato dextrose broth (PDB). After vigorous vortexing, cells were plated onto complete medium (CM; ref. 13) to isolate meiotic progeny. For the isolation of double-resistant progeny (drp), cells were plated on CM agar containing both hygromycin B (300 μg/ml, Rose Scientific, Edmonton, Canada) and phleomycin (20 μg/ml, Cayla Laboratories, Toulouse, France). Isolated colonies were picked and resuspended in sterile water. The suspension was vortexed for 5 min and spread onto CM agar containing hygromycin B and phleomycin. Isolated colonies then were grown in PDB for mating tests and for DNA isolation.

Results

The *a* and *b* Gene Complexes Are Separated by Large Physical Distances in *MAT-1* and *MAT-2* Strains. Initially, we sought to determine the physical distance between the *a* and *b* gene complexes within the *MAT-1* and *MAT-2* loci of *U. hordei*. We constructed strains that were tagged with the recognition sequence of the rare-cutting restriction enzyme I-*Sce*I at the *a1* gene complex (364–86), the *b2* gene complex (365–57), or both the *a* and *b* gene complexes (364–86dt21 and 365–57dt51; Table 1, Fig. 1). Pulse-field gel electrophoresis and subsequent hybridization analysis of I-*Sce*I-digested chromosome-sized DNA from the double-tagged strains revealed two different-sized fragments

GENETICS

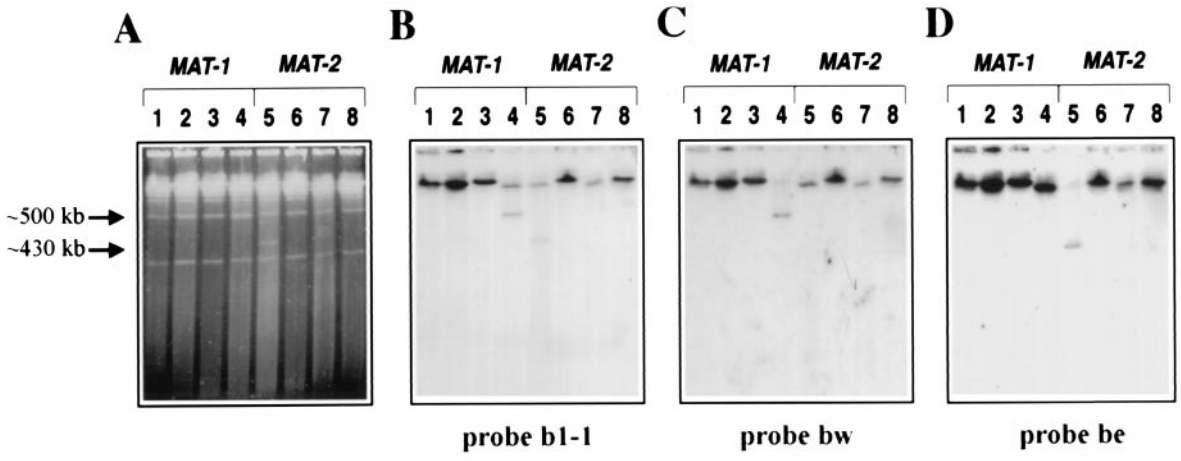

Fig. 2. Determination of the size and organization of the *MAT* locus of *U. hordei* by hybridization with probes from the *b* gene complex. (*A*) Ethidium-bromide-stained CHEF gel. (*B–D*) DNA gel blots of the same gel hybridized with the probes indicated. Lane 1, I-*Sce*I-digested 4857–4 (*a1b1*); lane 2, I-*Sce*I-digested 364–86 (*a1b1*; single tag at *a1*); lane 3, undigested 364–86dt21 (*a1b1*; double tag at *a1*, *b1*); lane 4, I-*Sce*I-digested 364–86dt21 (*a1b1*; double tag at *a1*, *b1*); lane 5, I-*Sce*I-digested 365–57dt51 (*a2b2*; double tag at *a2*, *b2*); lane 6, undigested 365–57dt51 (*a2b2*; double tag at *a2*, *b2*); lane 7, I-*Sce*I-digested 365–57 (*a2b2*; single tag at *b2*); lane 8, I-*Sce*I-digested 4857–5 (*a2b2*). Note that probes b1–1, be and bw recognize homologous sequences in both *MAT* loci.

representing the regions between *a* and *b* for the *MAT-1* and *MAT-2* strains (Fig. 2). A fragment of ≈500 kb was released upon digestion of DNA from the *MAT-1* double-tagged strain. This band comigrated with a 500-kb chromosome and appeared as a doublet in the gel stained with ethidium bromide (Fig. 2*A*, lane 4). Hybridization with probes from the *a* and *b* gene complexes confirmed that this DNA fragment originated from the *MAT-1* locus (Figs. 2 *B* and *C*, lanes 4, and 3*B*, lane 4). Similarly, digestion of the double-tagged *MAT-2* strain (365–57dt51) with I-*Sce*I released a fragment of ≈430 kb (Fig. 2*A*, lane 5). This fragment originated from the *MAT-2* locus as determined by hybridization with probes from both the *a* and *b* gene complexes (Figs. 2 *B* and *D*, lane 5, and 3*E*, lane 5).

The *MAT* Locus Is in the Center of a 2.8-Mb Chromosome. The DNA from wild-type, single-tagged, and double-tagged strains was subjected to pulse-field gel electrophoresis for an extended time to position the *MAT* locus on the chromosome. Interestingly, both *MAT-1* and *MAT-2* are situated in the central region of an ≈2.8-Mb chromosome (Fig. 1). In *MAT-1* strains, probe be hybridized to ≈1.6- and ≈1.1-Mb fragments released upon digestion of DNA from the strain tagged only at the *a1* locus and from the strain tagged at both *a1* and *b1*, respectively (Fig. 4*D*, lanes 2 and 4; see Fig. 1*A*). As expected, the bw probe hybridized to the same 1.6-Mb fragment released from the single-tagged strain and to the ≈500-kb fragment released from the double-tagged strain (Figs. 4*C*, lanes 2 and 4, and 2*C*, lane 4). These data

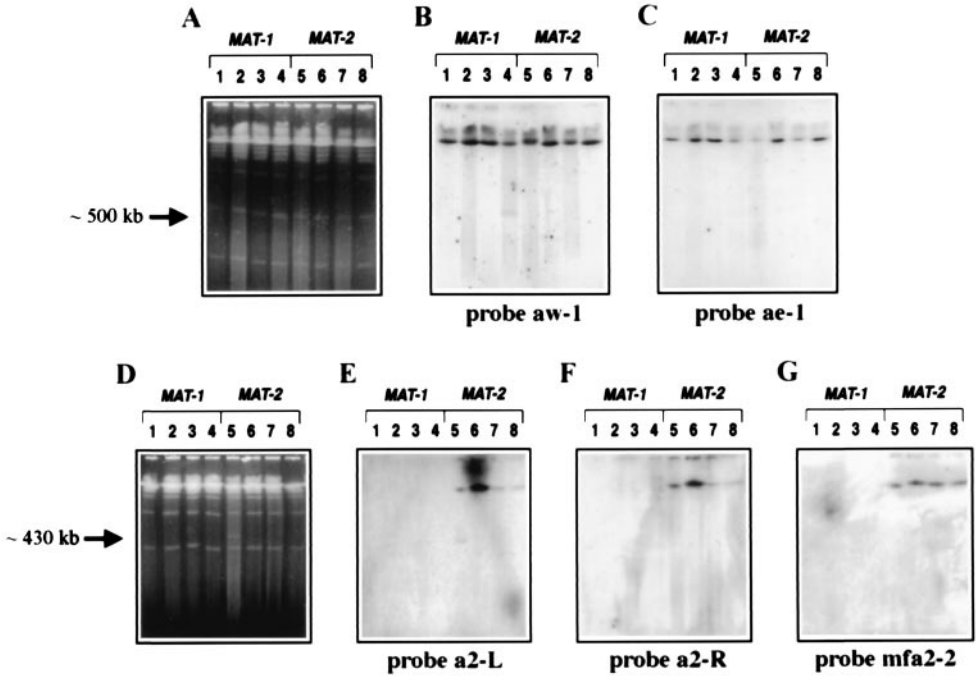

Fig. 3. Determination of the size and organization of the *MAT* locus of *U. hordei* by hybridization with probes from the *a* gene complex. (*A* and *D*) Ethidium-bromide-stained CHEF gels. (*B*, *C*, and *E*--*G*) DNA gel blots of the corresponding gels hybridized with the probes as indicated. Lanes are as described in Fig. 2.

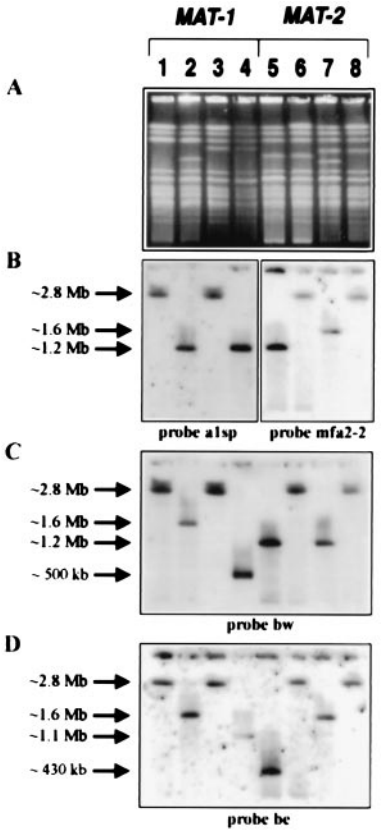

Fig. 4. Determination of the chromosomal position of the *MAT* locus by hybridization with probes from the *a* and *b* gene complexes. (*A*) Ethidium-bromide-stained CHEF gel. (*B–D*) DNA gel blots of the corresponding gels hybridized with the probes as indicated. Lanes are as described in Fig. 2.

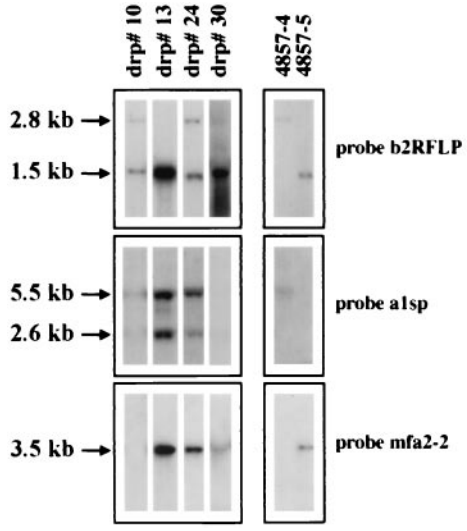

Fig. 5. Identification of mating-type-specific sequences in the drp by hybridization with probes from the *a* and *b* gene complexes. DNA gel blots of *Bam*HI-digested genomic DNA from representative drp (see text) and both parental strains were hybridized with the probes indicated.

confirmed that the *a1* and *b1* gene complexes are separated by ≈500 kb (Figs. 2 and 3). The hybridization of an ≈1.2-Mb fragment with probe a1sp showed that the *MAT-1* locus is centrally located, with ≈1.2 and ≈1.1 Mb flanking the *a1* and *b1* gene complexes, respectively (Figs. 4*B*, lanes 2 and 4, and 1*A*). Similar results were obtained for *MAT-2* strains. For example, probe be detected the 1.6-Mb fragment from the single-tagged strain and the 430-kb fragment from the double-tagged strain (Figs. 4*D*, lanes 5 and 7, and 1*B*). Furthermore, both probes mfa2–2 and bw hybridized to ≈1.2-Mb fragments released from the strain tagged at both *a2* and *b2*, revealing that the *MAT-2* locus also is located in the middle of an ≈2.8-Mb chromosome (Fig. 4 *B* and *C*, lane 5).

The 430- and 500-kb fragments were not detected by hybridization of any probe to the DNA of wild-type strains digested with I-*Sce*I, digested DNA from the single-tagged strains and undigested DNA from the double-tagged strains (Figs. 2 *B–D* and 3 *B*, *C*, *E*, and *F*, lanes 1–3 and 6–8). In fact, for all hybridizations, all of the probes hybridized to high molecular weight DNA shown to be the ≈2.8-Mb chromosome from wild-type and undigested double-tagged strains only (Figs. 2–4). We conclude that the 430-and 500-kb DNA fragments were indeed the regions between the *a* and *b* gene complexes.

The *a* and *b* Gene Complexes Have Different Organizations Within *MAT-1* and *MAT-2*. Hybridization with probes from either side of the I-*Sce*I site inserted at *b* revealed that the sequences at this gene complex in the *MAT-1* strain were inverted compared with the homologous sequences in the *MAT-2* strain. Both the bw and be probes contain homologous DNA sequences from the *b1* and *b2* gene complexes (Fig. 1; ref. 2). The bw probe hybridized to the 500-kb fragment that was released upon I-*Sce*I digestion of DNA from the double-tagged *MAT-1* strain, whereas probe be hybridized to the 430-kb fragment released upon digestion from the double-tagged *MAT-2* strain (Figs. 1 and 2 *C*, lane 4 and *D*, lane 5). These results indicate that the *bW* gene is closer to the *a* locus than the *bE* gene in *MAT-1* strains, and the orientation of *bE* and *bW* is reversed in *MAT-2* strains (Fig. 1).

Hybridization probes from both sides of the I-*Sce*I site at *a1* and *a2* were used to explore the overall organization of the *a* and *b* gene complexes within *MAT-1* and *MAT-2*. The aw-1 probe hybridized to the 500-kb region between *a1* and *b1*, indicating that the direction of transcription of *pra1* is oriented away from the *b1* gene complex (Figs. 1*A* and 3*B*, lane 4; ref. 17). In support of this conclusion, probe ae-1 hybridized to a higher molecular weight fragment shown to be ≈1.2-Mb (Figs. 1*A* and 3*C*, lane 4; comparable with probe a1sp in Fig. 4*B*, lanes 2 and 4). For *MAT-2*, the fragment from the 3′ terminus of *pra2* (probe a2-L, Fig. 1*B*) hybridized to the 430-kb fragment released after digestion with I-*Sce*I (Fig. 3*E*, lane 5). Accordingly, the probe from the 5′ end of *pra2* (probe a2-R, Fig. 1*B*) hybridized only to the higher molecular weight fragment shown to be ≈1.2 Mb (Fig. 3*F*, lane 5; comparable with probe mfa2–2 in Fig. 4*B*, lane 5). In addition, the hybridization with probe mfa2–2 (Fig. 1*B*) showed that *mfa2* was located upstream of *pra2* and outside of the 430-kb region spanning *pra2* and the *b* gene complex (Fig. 3*G*, lane 5). The organization of the *pra* and *mfa* genes at both *a1* and *a2* also has been confirmed by PCR and sequence analysis (17). Overall, our results show that the organization of the genes at *a1* differs from that of *a2*; i.e., *pra1* and *mfa1* are convergently transcribed and *pra2* and *mfa2* are divergently transcribed.

Interestingly, the probes from the flanking sequences of the I-*Sce*I site at the *a2* gene complex (a2-L, a2-R, and mfa2–2; Fig. 1*B*) did not hybridize to DNA from *MAT-1* strains (Figs. 3 *E* and *F*, lanes 1–4, and 4*B*). Probe a1sp, containing the *pra1* gene, was also specific for *MAT-1* strains (Figs. 4*B* and 5). These results indicate that regions of nonhomology may exist between the *a* gene complexes in *MAT-1* and *MAT-2*.

Recombination Is Suppressed in the Region Between *a* and *b*. In previous work, a screen of 2,000 progeny failed to identify strains

Table 2. Segregation of markers in crosses to detect recombination within *MAT*

Cross	Ratio of progeny with the following genotypes: *MAT-1*/ *MAT-2**	*phleo*^{r}/ *phleo*^{s}†	*hyg*^{s}/ *hyg*^{r}†	*phleo*^{r}, *hyg*^{r}/ *phleo*^{s}, *hyg*^{s}‡
1	24/25	24/25	24/25	6/18,400
2	23/26	23/26	23/26	7/18,400
3	26/24	26/24	26/24	10/17,800
4	35/15	35/15	35/15	11/17,400
Total	108/90	108/90	108/90	34/72,000

*The genotypes of the progeny were determined by performing mating tests with wild-type strains 4857-4 and 4857-5.

†Two hundred random progeny were tested for resistance to phleomycin (*phleo*^{r}) or hygromycin B (*hyg*^{r}).

‡For each cross, 20, 000 progeny were inoculated onto culture medium. An average viability of ~90% was obtained for each cross. A total of 72,000 viable progeny were tested for resistance to both antibiotics. A second trial identified 36 progeny (out of 70,420) that were resistant to both antibiotics.

with altered mating types caused by recombination within the *MAT* locus (3). To further investigate the apparent low frequency of recombination in the region between *a* and *b*, the gene complexes were tagged with genes for resistance to the antibiotics phleomycin and hygromycin B. Specifically, two strains were constructed by insertion of the phleomycin gene at the *a1* locus (364–62 and 364–86) and two strains were obtained with the hygromycin B gene at the *b2* locus (365–57 and 365–71) (Fig. 1, Table 1).

The *a1*-tagged strains each were crossed with the two strains tagged at *b2* by coinoculation of barley seedlings. Our goal was to estimate the frequency of recombination between the *a* and *b* gene complexes by germinating the teliospores from the crosses and selecting double-resistant recombinant progeny on a medium with both antibiotics. Presumably, only progeny having the recombinant genotype *a1b2* (*phleo*^{r}, *hyg*^{r}) would be able to form colonies, and their frequency of appearance would provide a measure of recombination.

Initially, 50 meiotic progeny were isolated from each of the four crosses. The mating type specificities of these strains were determined by plate-mating assays with two wild-type strains, 4857–4 *(a1b1)* and 4857–5 (*a2b2*). These progeny also were tested for resistance to phleomycin and hygromycin B. As shown in Table 2, mating type and antibiotic resistance segregated in an approximately 1:1 fashion in three of the four crosses; the fourth cross showed a reduced recovery of *MAT-2*, *phleo*^{s}, *hyg*^{r} progeny for unknown reasons. As expected, the progeny demonstrated complete linkage between phleomycin resistance and *MAT-1* mating specificity and between hygromycin B resistance and *MAT-2*. Overall, the analysis of the 200 progeny from these crosses indicated that meiotic segregation occurred normally in the strains carrying tagged *a1* and *b2* sequences.

To determine the frequency of recombination between the *a* and *b* gene complexes, a total of 72,000 isolates from the four crosses were plated on a medium containing both antibiotics. Considering the number of germinated spores used and the number of progeny per spore (average of 12), we estimated that our sample represented between 10,000 and 20,000 random progeny. The selection for drp yielded only 34 colonies, suggesting that recombination was indeed greatly suppressed within the *MAT* region despite the 400- to 500-kb distance separating *a* and *b*. The 34 drp subsequently were tested for their mating specificity in assays with two wild-type strains (4857–4 and 4857–5) and four strains engineered with artificial combinations of *a* and *b* (549, 550, 551, and 552; Table 1; ref. 11). Interestingly, none of the drp mated solely with the 549 or 550 tester strains, and the majority displayed unusual mating behaviors. Although numerous independent mating tests were performed, most of the progeny either failed to consistently give a positive mating reaction with any tester strain or mated routinely with more than one tester (data not shown).

The possibility that the drp contained both selectable markers because of the maintenance of both parental copies of the *MAT* chromosome rather than recombination was explored by a molecular test for the presence of the *a* and *b* gene complexes from both *MAT-1* and *MAT-2*. Representative hybridization results are shown in Fig. 5. Specifically, the b2RFLP hybridization probe was used to detect a restriction fragment length polymorphism (RFLP) that segregates with mating type (Figs. 1*B* and 5; ref. 10). Hybridization of this probe to DNA from the progeny revealed that many (13/34) contained both RFLP fragments, indicating the presence of both *b1* and *b2*. Interestingly, hybridization with *a1*- and *a2*-specific probes revealed that most of the drp (32/34) contained both *a1*- and *a2*-specific sequences (Fig. 5). In addition, all of the drp carrying *a1*-specific sequences showed an unusual hybridization pattern in that both a wild-type fragment of 5.5 kb and a unique 2.6-kb fragment hybridized to probe a1sp (Fig. 5). Possibly, the extra fragment arose from a recombination event that resulted in a duplication of part of the *pra1* gene. Overall, the molecular markers demonstrated in Fig. 5 were found in the following combinations in the 34 progeny: *a1*, *b1*, *b2* (1/34; e.g., drp#10); *mfa2*, *b1*, *b2* (1/34; e.g., drp#30); *a1*, *mfa2*, *b1*, *b2* (11/34; e.g., drp#24); *a1*, *mfa2*, *b2* (21/34; e.g., drp#13). In summary, these results indicated that the double-resistant phenotype was not the result of a simple reciprocal recombination event between *a* and *b* in the 34 drp analyzed. Rather, the drp most likely arose from other events such as rearrangements at *a* or *b* or the retention of all or part of both *MAT* chromosome homologues to yield aneuploid, or perhaps, diploid strains. It also should be noted that true reciprocal recombinant progeny from our experiments may have been inviable and therefore not detected, although *a1b2* and *a2b1* strains have been constructed (11).

Discussion

The *MAT* Locus of *U. hordei* Is Larger Than Previously Characterized Fungal Mating Type Loci. Our experiments indicate that the *MAT* locus for *U. hordei* is surprisingly large compared with the mating-type sequences characterized in other fungi (18). Among fungi, the largest mating-type regions have been described in basidiomycetes. For example, the mushroom *Coprinus cinereus* possesses mating-type loci of approximately 30 kb (*A42* locus) and 17 kb (*B6* locus) (19, 20). The *A* and *B* loci of *C. cinereus* encode proteins with functional similarity to the *b*- and *a*-encoded proteins of *U. hordei*, respectively. The *MAT* locus of the human pathogen *Cryptococcus neoformans* is 35–45 kb in size, although it has been suggested recently that the locus may be as large as 75 kb (21, 22). This locus has been implicated in virulence (23).

In the context of pathogenicity, the large size and multigenic nature of the *MAT* locus of *U. hordei* is reminiscent of complex pathogenicity regions that segregate as one locus in other phytopathogenic fungi. For example, the *Tox2* locus of *Cochliobolus carbonum* is responsible for the production of a host-specific toxin, which promotes lesion formation on leaves of susceptible host plants. The genetic functions for toxin synthesis segregate as a single unit, although *Tox2* spans a region of >500 kb (24). In *Nectria haematococca*, the genes required for pathogenicity to pea (*PEP*) have been localized to a dispensable chromosome that is proposed to be suppressed for recombination (25). Furthermore, genes involved in the biosynthesis of elicitins are clustered in *Phytophthora cryptogea*, as are mycotoxin biosynthetic genes in *Fusarium* species, *Aspergillus nidulans*, and *Gibberella fujikuroi* (26–29). These examples make it

tempting to speculate that other genes involved in mating and pathogenesis might be clustered along with the *a* and *b* genes at the *MAT* locus of *U. hordei*. In other words, recombination suppression may serve to maintain a set of genes together that function in the sexual development of the fungus in the host. Further characterization of the sequences between *a* and *b* will elucidate the organization of this region, show the relationship between *MAT-1* and *MAT-2,* and, perhaps, reveal additional genes involved in mating and pathogenesis.

Recombination on the *MAT* Chromosome of *U. hordei*. Although recombination was investigated only in the region between the *a* and *b* gene complexes in this study, it is conceivable that regions outside of these gene complexes may be suppressed for recombination as well. Precedent exists for suppression extending over large distances in fungi, e.g., the absence of recombination between several loci spanning almost the entire chromosome carrying the mating-type locus has been reported for *Neurospora tetrasperma* (30). Very few genetic markers have been identified in *U. hordei,* and it is therefore difficult to assess the relationship between physical and genetic distance over any portion of the genome. A limited number of studies have explored recombination between the *MAT* locus and linked markers, and these indicate that crossing over occurs on the *MAT* chromosome. For example, Groth (31) reported a recombination frequency of 10.8% between *MAT* and a gene conditioning a mycelial phenotype for haploid cells. In addition, Henry *et al.* (32) reported a recombination frequency of 12% for the *pan-1* and *pro-2* genes in *U. hordei*; the *pan-1* gene is known to be located within or near the *a* gene complex in both *U. hordei* (Fig. 1*A*) and *U. maydis* (5). Thomas (33) examined recombination between the *MAT* locus, *pan1*, and *pro1* among 361 ordered tetrads of *U. hordei*. All but eight tetrads had the parental combination of markers indicating tight linkage of all three traits. The remaining eight tetrads showed unusual segregation for one or more of the markers (e.g., 3:1 and 4:0 ratios) suggesting that gene conversion events may have occurred. In fact, two of these tetrads segregated 3:1 for *MAT*. In general, further characterization of the *MAT* locus will require additional physical and genetic mapping to generate a more detailed picture of recombination frequencies across the chromosome and to clarify the actual size of the *MAT* locus.

Does *U. hordei* Possess Primitive Dimorphic Sex Chromosomes? The features of the *MAT* locus such as recombination suppression, insertion/deletions, inversion, regions of nonhomology between *MAT-1* and *MAT-2*, and the presence of sex-determining genes, are reminiscent of the X/Y sex-chromosome systems (34–36). A striking similarity between the mating system of the lower eukaryote *Chlamydomonas reinhardtii* and sex chromosomes in higher eukaryotes already has been described (36, 37). Intrachromosomal translocations, inversions, duplications, and large deletions are associated with the *mt* locus and are thought to contribute to the suppression of recombination within a 830-kb stretch of DNA (37). Suppression of recombination at mating-type loci has been attributed to a variety of mechanisms including nonhomology of genes at the locus, different complements of genes, chromosomal rearrangements, or a special chromatin structure (18, 37). The *MAT* locus of *U. hordei* appears to share features with the *mt* locus of *C. reinhardtii* that may contribute to suppressed recombination, although a more detailed characterization of the *U. hordei* locus is needed. In particular, it will be of interest to search the *MAT* locus for additional features that may shed light on the evolution of sex chromosomes, such as repetitive sequences and transposable elements (36, 37). This search also will enhance our understanding of the mechanism by which recombination is suppressed between *MAT-1* and *MAT-2*; it may be the case, for example, that recombination suppression within the centrally located *MAT* locus may be caused by the presence of the centromere. Further analysis of the chromosomes carrying *MAT* in *U. hordei* may contribute to an understanding of the evolution of dimorphic sex chromosomes and mating-type loci in fungi.

We thank Dr. Percy Thomas for *U. hordei* strains and Deborah Willits for technical assistance. This work was supported by the Natural Sciences and Engineering Research Council of Canada (J.W.K.) and the U.S. Department of Agriculture/National Research Initiative (#94–37303–0765; J.E.S.).

1. Thomas, P. L. (1988) *Adv. Plant Pathol.* **6,** 415–425.
2. Bakkeren, G. & Kronstad, J. W. (1993) *Plant Cell* **5,** 123–136.
3. Bakkeren, G. & Kronstad, J. W. (1994) *Proc. Natl. Acad. Sci. USA* **91,** 7085–7089.
4. Rowell, J. B. & DeVay, J. E. (1954) *Phytopathology* **44,** 356–362.
5. Froeliger, E. H. & Leong, S. A. (1991) *Gene* **100,** 113–122.
6. Bölker, M., Urban, M. & Kahmann, R. (1992) *Cell* **68,** 441–450.
7. Puhalla, J. E. (1968) *Genetics* **60,** 461–474.
8. Gillissen, B., Bergemann, J., Sandmann, C., Schroeer, B., Bölker, M. & Kahmann, R. (1992) *Cell* **68,** 647–657.
9. Kämper, J., Reichmann, M., Romeis, T., Bölker, M. & Kahmann, R. (1995) *Cell* **81,** 73–83.
10. Bakkeren, G., Gibbard, B., Yee, A., Froeliger, E. H., Leong, S. A. & Kronstad, J. W. (1992) *Mol. Plant-Microbe Interact.* **5,** 347–355.
11. Bakkeren, G. & Kronstad, J. W. (1996) *Genetics* **143,** 1601–1613.
12. Martinez-Espinoza, A. D., Gerhardt, S. A. & Sherwood, J. E. (1993) *Exp. Mycol.* **17,** 200–214.
13. Holliday, R. (1974) in *Handbook of Genetics*, ed. King, R. C. (Plenum, New York), Vol. 1, pp. 575–595.
14. Kronstad, J. W. & Leong, S. A. (1990) *Genes Dev.* **4,** 1384–1395.
15. Gold, S., Bakkeren, G., Davies, J. E. & Kronstad, J. W. (1994) *Gene* **142,** 225–230.
16. Thierry, A. & Dujon, B. (1992) *Nucleic Acids Res.* **20,** 5625–5631.
17. Anderson, C. M., Willits, D. A., Kosted, P. J., Ford, E., Martinez-Espinoza, A. D. & Sherwood, J. E. (1999) *Gene* **240,** 89–97.
18. Kronstad, J. W. & Staben, C. (1997) *Annu. Rev. Genet.* **31,** 245–267.
19. Kües, U., Asante-Owusu, R. N., Mutasa, E. S., Tymon, A. M., Pardo, E. H., O'Shea, S. F., Göttgens, B. & Casselton, L. A. (1994) *Plant Cell* **6,** 1467–1475.
20. O'Shea, S. F., Chaure, P. T., Halsall, J. R., Olesnicky, N. S., Laibbrandt, A., Connerton, I. F. & Casselton, L. A. (1998) *Genetics* **148,** 1081–1090.
21. Moore, T. D. E. & Edman, J. C. (1993) *Mol. Cell. Biol.* **13,** 1962–1970.
22. Wickes, B. L., Edman, U. & Edman, J. C. (1997) *Mol. Microbiol.* **26,** 951–960.
23. Kwon-Chung, K. J., Edman, J. C. & Wickes, B. L. (1992) *Infect. Immun.* **60,** 602–605.
24. Ahn, J.-H. & Walton, J. (1996) *Plant Cell* **8,** 887–897.
25. VanEtten, H., Wasmann, C. & McCluskey, K. (1994) in *Advances in Molecular Genetics of Plant-Microbe Interactions*, eds. Daniels, M. J., Downie, J. A. & Osbourn, A. E. (Kluwer, Dordrecht, The Netherlands), Vol. 3, pp. 163–170.
26. Panabières, F., Marais, A., Le Berre, J.-Y., Penot, I., Fournier, D. & Ricci, P. (1995) *Mol. Plant-Microbe Interact.* **8,** 996–1003.
27. Desjardins, A. E., Hohn, T. M. & McCormick, S. P. (1993) *Microbiol. Rev.* **57,** 595–604.
28. Desjardins, A. E., Plattner, R. D. & Proctor, R. H. (1996) *Appl. Environ. Microbiol.* **62,** 2571–2576.
29. Brown, D. W., Yu, J.-H., Kelkar, H. S., Fernandes, M., Nesbitt, T. C., Keller, N. P., Adams, T. H. & Leonard, T. J. (1996) *Proc. Natl. Acad. Sci. USA* **93,** 1418–1422.
30. Merino, S. T., Nelson, M. A., Jacobson, D. J. & Natvig, D. O. (1996) *Genetics* **143,** 789–799.
31. Groth, J. V. (1975) *Can. J. Bot.* **53,** 2233–2239.
32. Henry, C. E., Bullock, B., Smith, V. & Steward-Clark, E. (1988) *Bot. Gaz.* **149,** 101–106.
33. Thomas, P. L. (1991) *Annu. Rev. Phytopathol.* **29,** 137–148.
34. Jablonka, E. & Lamb, M. J. (1990) *Biol. Rev. Camb.* **65,** 249–276.
35. Charlesworth, B. (1991) *Science* **251,** 1030–1033.
36. Charlesworth, B. (1994) *Curr. Biol.* **4,** 739–741.
37. Ferris, P. J. & Goodenough, U. W. (1994) *Cell* **76,** 1135–1145.